Supplementary Materials:

DNA "Nano-Claw": Logic-based Autonomous Cancer Targeting and Therapy

Mingxu You,[†,‡] Lu Peng,[‡] Na Shao,[‡] Liqin Zhang,[‡] Liping Qiu,[†] Cheng Cui,[‡] and Weihong Tan[†,‡]*

[†] Molecular Science and Biomedicine Laboratory, State Key Laboratory of Chemo/Bio-Sensing and Chemometrics, College of Chemistry and Chemical Engineering, College of Biology, Collaborative Innovation Center for Chemistry and Molecular Medicine, Hunan University, Changsha 410082, China

[‡] Department of Chemistry and Physiology and Functional Genomics, Center for Research at the Bio/Nano Interface, Shands Cancer Center, UF Genetics Institute, McKnight Brain Institute, University of Florida, Gainesville, FL 32611-7200, USA Fax: (+1)352-846-2410

*Correspondence to: tan@chem.ufl.edu

Within this supporting information are found:

1. **Experimental Section**

2. **Supplementary Tables**

3. **Supplementary Figures and Notes**

1. **Experimental Section:**

Chemicals, cell lines and reagents. The materials for DNA synthesis were purchased from Glen Research (Sterling, VA), including 6-(3',6'-dipivaloylfluoresceinyl-6-carboxamido)-hexyl-phosphoramidite (6-FAM) and 5'-amino phosphoramidite. Photodynamic ligand chlorine e6 (Ce6) was purchased from Frontier Scientific, Logan, UT. Other chemicals were purchased from Sigma-Aldrich. HeLa cells were cultured in DMEM medium (Sigma), and CCRF-CEM (CCL-119, T-cell line, human ALL), Ramos (CRL-1596, B-cell line, human Burkitt's lymphoma) and K562 (CCL-240, acute promyelocytic leukemia, CML) were cultured in RPMI 1640 medium (American Type Culture Collection) with 10% fetal bovine serum (Invitrogen, Carlsbad, CA) and 0.5 mg/mL penicillin-streptomycin (American Type Culture Collection) at 37 °C under a 5% CO_2 atmosphere. Cells were washed before and after incubation with washing buffer [4.5 g/L glucose and 5 mM $MgCl_2$ in Dulbecco's PBS with calcium chloride and magnesium chloride (Sigma-Aldrich)]. Binding buffer was prepared by adding yeast tRNA (0.1 mg/mL; Sigma-Aldrich) and BSA (1 mg/mL; Fisher Scientific) to the washing buffer to reduce background binding. All reagents for buffer preparation and HPLC purification came from Fisher Scientific. Unless otherwise stated, all chemicals were used without further purification.

DNA synthesis. All oligonucleotides were synthesized using an ABI 3400 DNA synthesizer (Applied Biosystems, Inc., Foster City, CA) at the 1.0 micromole scale. After complete cleavage and deprotection, the DNA sequences were purified on a ProStar HPLC system (Varian, Palo Alto, CA) with a C-18 reversed-phase column (Alltech, 5 μm, 250 mm × 4.6 mm). The eluent was 100mM triethylamine-acetic acid buffer (TEAA, pH 7.5) and acetonitrile (0-30 min, 10-100%). All DNA concentrations were characterized with a Cary Bio-300UV spectrometer (Varian) using the absorbance of DNA at 260nm.

Synthesis of photosensitizer-modified oligonucleotides. Using 5'-end Ce6 modified strand as an example, the 5'-amino-modified oligonucleotide was synthesized and the MMT protection group removed using an ABI 3400 DNA synthesizer in order to conjugate the carboxyl group with the Ce6 molecule. To improve the coupling efficiency and reduce the multiple coupling products, the amount of Ce6 was 10 times that of the oligonucleotides in the coupling reaction. In a typical reaction, 10 μmole Ce6 was mixed with an equivalent amount of coupling agents, N,N'-Dicyclohexylcarbodiimide (DCC) and N-Hydroxysuccinimide (NHS), in 500 μL N,N-Dimethylformamide (DMF) for the activation reaction. The product was then washed with acetonitrile until clear, dried using a vacuum dryer, and further purified by reversed-phase HPLC.

Manipulation of the AND and INH logic gates. The preannealed DNA duplex was prepared by a cooling process from 95 to 4 °C over 30 min in a 12 mM PBS buffer (pH=7.4 with 137 mM NaCl and 2.7 mM KCl); other DNA probes were cooled on ice for 10 min before usage. Tagged aptamer probes were incubated at a concentration of 200 nM with 10^6 cells per mL in 200 μL binding buffer and shaken on ice for 30min. After washing and discarding the nonbinding probes, 200 nM FAM-labeled reporter probe or duplex was added for 1 hour of strand binding and incubation on ice. After further washing to remove nonbinding probes, the final detection of cellular fluorescence signal was performed with a FACScan cytometer (Becton Dickinson Immunocytometry Systems, San Jose, CA) by counting 20 000 events, using channel #3 for the FAM dye and channel #5 for the PE-Cy5.5 dye.

Photodynamic therapy and cell viability test. The cell viability of different cell lines was determined using the propidium iodide (PI) staining assay (Molecular Probes Inc., Eugene, OR). At first, the cells (100k cells/well) were incubated with the logic machines following the above-mentioned method. For photodynamic therapy, the cells were separately placed in a 48-well plate

on ice for 3 hours irradiation with white light (15 W, 60 Hz table lamp). After irradiation, the cells were incubated in culture medium at 37 °C under 5% CO_2 atmosphere for further cell growth (48 h). To measure the cell viability, 1.5 μL PI (10-fold dilution from 1.0 mg/mL water solution) was added to each well and incubated for 15 min at room temperature before analyzing cells on the flow cytometer. Ten thousand events were counted for each well, using channel #4 for the PI dye.

The construction of DNA "Nano-Claw". The scaffold sequences of the trivalent "Y"-shaped and tetravalent "X"-shaped DNA nanostructures have been reported before.[1,2] The preannealed scaffold-effector toe conjugate and capture toes were separately prepared by a slower cooling process from 95 to 25 °C over 8 hours in a 12 mM PBS buffer, then mixed together to form the "Nano-Claw". Each nanostructure for different gates was separately purified from a gel electrophoresis experiment. The gel was run in 10% acrylamide (containing 19/1 acrylamide/bisacrylamide) mixture with $1\times$ TBE/15 mM Mg^{2+} buffer, at 100 V constant voltage for 3 hours (4 °C). Such gel purification process allowed the removal of partially assembled structures and decreased the false-positive signals. After purification, the concentrations of DNA nanostructures were characterized with a Cary Bio-300 UV spectrometer (Varian) using the absorbance of DNA at 260 nm. The extinction coefficients for the formed nanostructures were calculated from the equation:[3] $\varepsilon_{ds} = \varepsilon_{ss}(str1) + \varepsilon_{ss}(str2) - 3200 \times N_{AT} - 2000 \times N_{GC}$, where $\varepsilon_{ss}(str1)$ and $\varepsilon_{ss}(str2)$ are the extinction coefficient of each component single strand in the duplex, and N_{AT} and N_{GC} are the number of A-T and G-C pairs in the duplex form, respectively.

The operation of DNA "Nano-Claw". After purification, the prepared claw conjugation was then incubated at a concentration of 200 nM with 10^6 cells/ mL in binding buffer at room temperature with shaking for the first 30 min. The strand displacement was allowed to occur

over another 3 or 4 hours for the "Y"-shaped claw and "X"-shaped claw, respectively. After a further washing step to remove nonbinding probes, the final detection of cellular fluorescence signal was performed with a FACScan cytometer by counting 20 000 events, using channel #3. For the photodynamic therapy studies, the Ce6 photosensitizer and BHQ-3 quencher modified strands were used for the construction of Nano-Claw, and the cell viability of different cell lines was determined using the propidium iodide (PI) staining assay, as detailed above.

2. **Supplementary Tables:**

Table S1: DNA sequences for structure-switchable aptamers and 2-input logic gates.

Name	Sequence
cS_{11}	5'- TCTAACCGTAC-**FAM**-3'
cS_{15}	5'- (**Ce6**)-TCTAACCGTACAGTA-**FAM**-3'
cS_{19}	5'- TCTAACCGTACAGTATTTT-**FAM**-3'
Sgc8c	5'- ATCTAACTGCTGCGCCGCCGGGAAAATACTGTACGGTTAGA -3'
4f-0	5'- TTATCTCCTGTCCCC-**FAM**-3'
4f-1	5'- TCACTTATCTCCTGT-**FAM**-3'
4f-2	5'- TCACTTATCTCCTGTCCCC-**FAM**-3'
4f-3	5'- CTCGTTATAAGTGAT-**FAM**-3'
4f-4 (cF_{15})	5'- CGCACTCGTTATAAG-**FAM**-3'
4f-5	5'- CGCACTCGTTATAAGTGAT-**FAM**-3'
Sgc4f	5'- ATCACTTATAACGAGTGCGGATGCAAACGCCAGACAGGGGGACAGGAGATAAGTGA-Biotin -3'
Sgc4f-S_{15}	5'- ATCACTTATAACGAGTGCGGATGCAAACGCCAGACAGGGGGACAGGAGATAAGTGAAAAAA TACTGTACGGTTAGA -3'
TC-0 (cT_{15})	5'- ACCAAATGACGTTAG-**FAM**-3'
TC-1	5'- ATGACGTTAGAAGTC-**FAM**-3'
TC-2	5'- AGGTTGCATCTGTGT-**FAM**-3'
TC-3	5'- GCATCTGTGTTTGGT-**FAM**-3'
TC01	5'- ACCAAACACAGATGCAACCTGACTTCTAACGTCATTTGGT-Biotin -3'

Table S2: DNA sequences for constructing "Y"-shaped 2-input Nano-Claw.

Name	Sequence
Y01	5'- GGAATCACTGACATGTGGATCCGCATGACATTCGCCGTAAG -3'
Y02	5'- GGTACTATTGCATCTCTTACGGCGAATGACCGAATCAGCCT -3'
Y03	5'- GGTACGCAGTATTATAGGCTGATTCGGTTCATGCGGATCCA -3'
TC01-t(5,15,25)-Y01	5'- CATGTCAGTGATTCC-(ttttt)$_{1/3/5}$ - ACCAAACACAGATGCAACCTGACTTCTAACGTCATTTGGT -3'
Sgc4f-t(5,15)-Y01	5'- CATGTCAGTGATTCC-(ttttt)$_{1/3}$ - ATCACTTATAACGAGTGCGGATGCAAACGCCAGACAGGGGGACAGGAGATAAGTGA -3'
Sgc8-t(5,15,25)-Y02	5'- AGATGCAATAGTACC-(ttttt)$_{1/3/5}$ – ATCTAACTGCTGCGCCGCCGGGAAAATACTGTACGGTTAGA -3'
T'-Y01	5'- CATGTCAGTGATTCC TTTTT CTAACGTCATTTGGT -3'
S'-Y02	5'- AGATGCAATAGTACCTTTTT TACTGTACGGTTAGA -3'
R-Y03	5'- ATAATACTGCGTACCTTTTTTTACAGTAGATATGCC-**FAM** (or Biotin or **Ce6**) -3'
cS'	5'- TCTAACCGTACAGTAGATATGCC -3'
cT'	5'- CGGTTAGAACCAAATGACGTTAG -3'
S'	5'- **Dabcyl** (**BHQ-3**)-GGCATATCTACTGTACGGTTAGACGCACTC -3'
T'	5'- CTTATAACGAGTGCGTCTAACCG -3'

Table S3: DNA sequences for constructing "X"-shaped 3-input Nano-Claw.

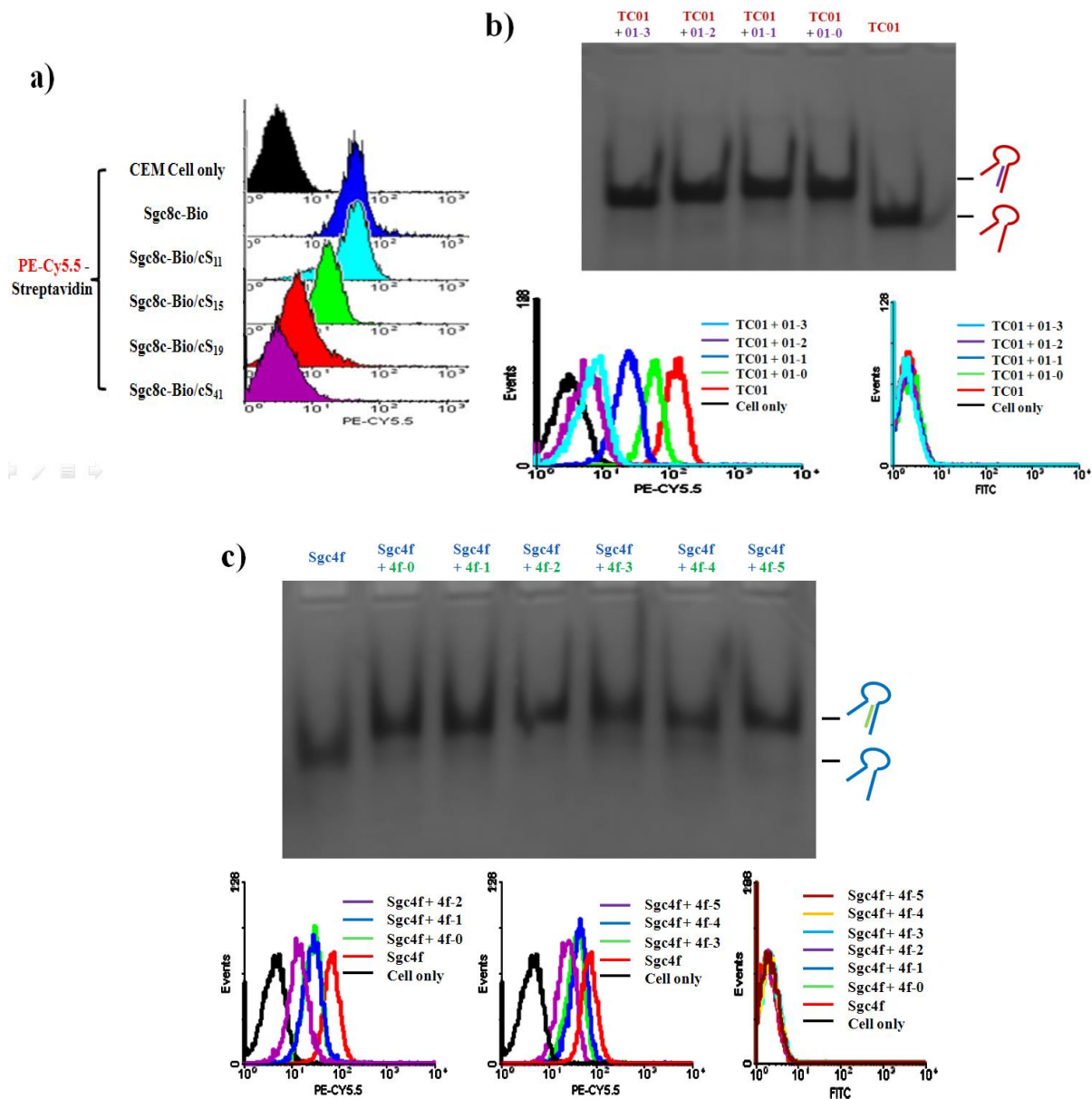| Name	Sequence
T01	5'- GGATAGCGCGTGATCGGAACGCCTACGATGGACACGCCGACC -3'
T02	5'- GGTCGGCGTGTGGTTGCGCTC -3'
T03	5'- GAGCGCAACCTCCCTGGCAAGACTCCAGAGGACTACTCATCC -3'
T04	5'- GGATGAGTAGTGGGCTCAGTC -3'
T05	5'- GACTGAGCCCTGCTAGGATCGACTTCACTGGACCGTTCTACC -3'
T06	5'- GGTAGAACGGTGGAAGCCAAC -3'
T07	5'- GTTGGCTTCCTGTACGGCAGAACTCCGTTGGACGAACACTCC -3'
T08	5'- GGAGTGTTCGTCGCGCTATCC -3'
T09	5'- AGGGACCATCGTAGGTTTTCGTTCCGATCACCAACGGAGTTTTTTCTGCCGT ACACCAGTGAAGTTTTTCGATCCTAGCACCTCTGGAGTTTTTCTTGCC -3'
TC01-t(5,15,25)-T02	5'- GGTCGGCGTGTGGTTGCGCTC-(ttttt)$_{1/3/5}$− ACCAAACACAGATGCAACCTGACTTCTAACGTCATTTGGT -3'
Sgc8-t(5,15,25)-T04	5'- GGATGAGTAGTGGGCTCAGTC-(ttttt)$_{1/3/5}$− ATCTAACTGCTGCGCCGCCGGGAAAATACTGTACGGTTAGA -3'
Sgc4f-t(5,15)-T08	5'- GGAGTGTTCGTCGCGCTATCC-(ttttt)$_{1/3}$− ATCACTTATAACGAGTGCGGATGCAAACGCCAGACAGGGGGACAGGAGATAAGTGA -3'
T*-T02	5'- GGTCGGCGTGTGGTTGCGCTCTTTTTT CTAACGTCATTTGGT -3'
S*-T04	5'- GGATGAGTAGTGGGCTCAGTCTTTTTT TACTGTACGGTTAGA -3'
F*-T08	5'- GGAGTGTTCGTCGCGCTATCCTTTTTT CTTATAACGAGTGCG -3'
R-T06	5'- GGTAGAACGGTGGAAGCCAACTTTTTTTACAGTAGATATGCC-**FAM**(or Biotin) -3'
S*	5'- **Dabcyl**-GGCATATCTACTGTACGGTTAGAACCAAAT -3'
F*	5'- ACGTTAGCTTATAACGAGTGCGTCTAACCG -3'
T*	5'- GTTATAAGCTAACGTCATTTGGT -3'
cS*	5'- TCTAACCGTACAGTAGATATGCC -3'
cF*	5'- CGGTTAGACGCACTCGTTATAAG -3'
cT*	5'- ACCAAATGACGTTAGCTTATAAC -3'

3. **Supplementary Figures:**

Figure S1. Determination of the best replacement sites within aptamers. The bands in the 10% native gel prove the duplex formation between aptamer and each studied short piece of candidate strand. In the flow cytometry experiment, the strands able to be replaced by the aptamer's binding with cell-surface marker will result in a high PE-Cy5.5 fluorescence signal (from biotin-labeled TC01, Sgc4f or Sgc8c aptamer) and a low (or no) FITC fluorescence signal (labeled on the candidate strands). The strong PE-Cy5.5 signal demonstrates that the formation of "aptamer/candidate" duplex will not prohibit the binding between the aptamer and cell-surface marker; meanwhile, the weak (or no) FITC signal proves that the candidate strand will be freed after cellular binding, instead of forming a "cell/aptamer/candidate strand" complex structure.
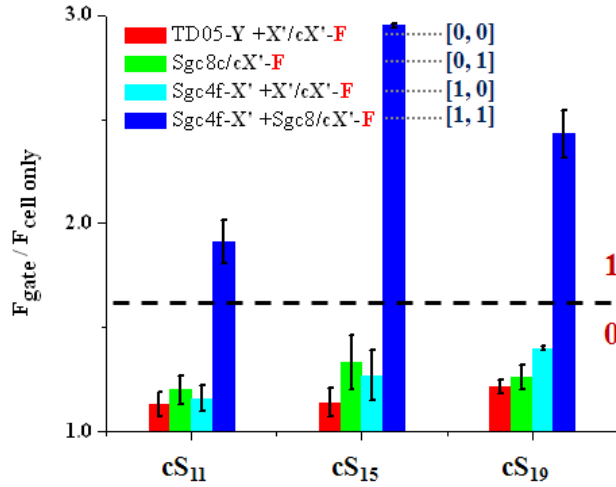
Figure S2. The influence of different sequence lengths of the cS probe on the AND gate efficiency. The longer cX' (i.e., cS) probe binds more strongly with Sgc8c aptamer for successful DNA strand displacement after cellular binding to activate the gate signal, requiring, in turn, a higher number of cell-surface PTK7 receptors. By adjusting the sequence length and concentration of the cX' probe, it is possible to fine-tune the gating condition. Specifically, if the cX' probe is too short (*e.g.*, cS_{11} probe), it cannot be totally rehybridized with the Sgc4f-X' probe, even after 100% displacement by PTK7, because of its weaker duplex binding strength, which results in a weak ON signal. On the other hand, if the cX' probe is too long (*e.g.*, cS_{19} probe), binding to cell-surface PTK7 will not be strong enough to completely displace the cX' probe from the Sgc8c/cX' complex, also producing a poor S/B ratio. In this study, cS_{15} probe was used for further experimentation, considering the optimized gating function. Fluorescence values and their error bars (mean ± s.d.) were calculated based on the FITC signal from channel #3 in flow cytometry from three experiments.

Based on the concentration-dependent DNA hybridization effect, the short cS_{11} probe and medium-long cS_{15} probe could not be fully rehybridized with the small number of tagged Sgc4f on the HeLa cell surface (OFF signal for HeLa); in contrast, the long cS_{19} probe (19 nt) was capable of binding with the small number of tagged surface Sgc4f (ON signal for HeLa). Meanwhile, the release of the longer cX' probe from the Sgc8c/cX' conjugate requires a higher number of cell-surface PTK7 molecules. This results in a leveling effect to produce similar fluorescence signals on both CEM ($Sgc8c^{++}/Sgc4f^{++}$) and HeLa ($Sgc8c^{+++}/Sgc4f^{+}$) cell surfaces.
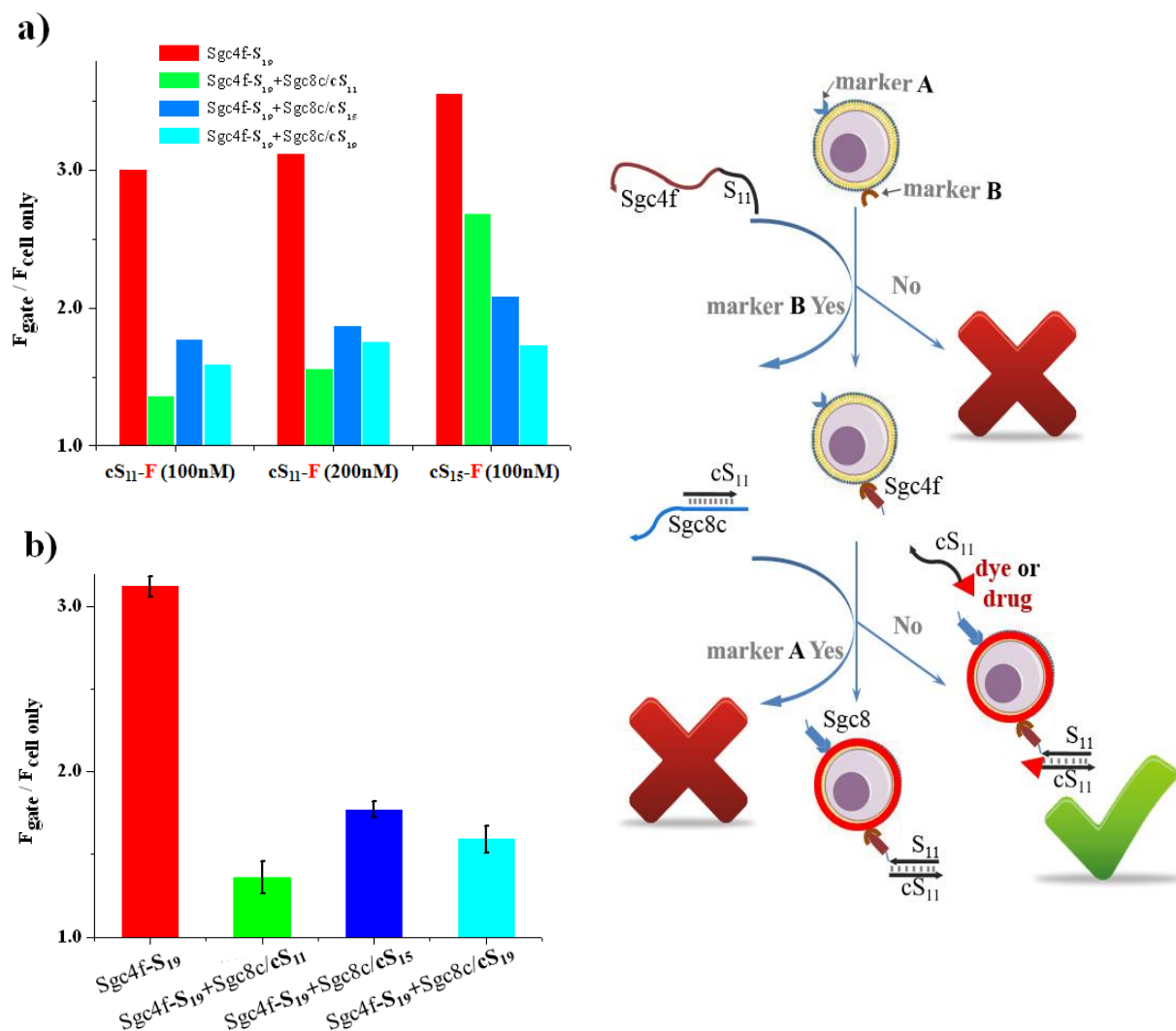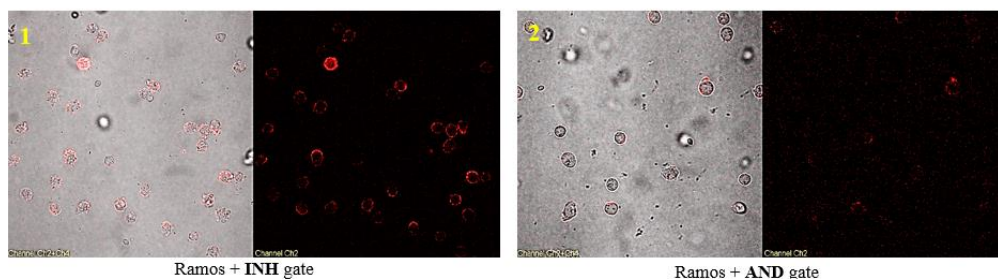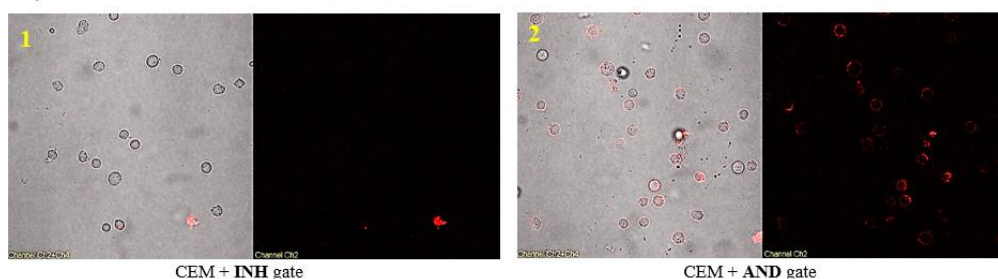
Figure S3. Optimization of the INH gate. (**a**) Different reporter sequences and concentrations were tested, and 100 nM cS_{11}-F was finally chosen as it had the best S/B ratio; (**b**) Sgc8c/cS_{11} complex was proven to be the best choice when using 100 nM cS_{11}-F as the reporter sequence. Right: experimental scheme of aptamer-switch INH gate.
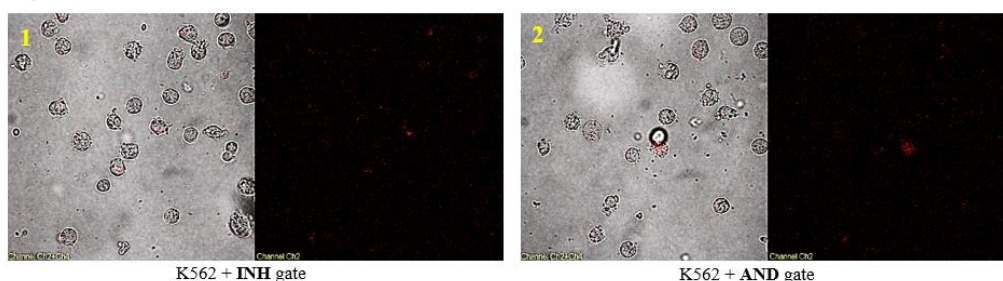
a) Ramos Cell

Ramos + **INH** gate

Ramos + **AND** gate

b) CEM Cell

CEM + **INH** gate

CEM + **AND** gate

c) K562 Cell

K562 + **INH** gate

K562 + **AND** gate

d) HeLa Cell

HeLa + **INH** gate

HeLa + **AND** gate

Figure S4. Fluorescence confocal microscopy images of the studied cell-surface logic sensors. The optical image (left) and fluorescence image (right) are shown after adding gating probes for (**a**) Ramos, (**b**) CEM, (**c**) K562 and (**d**) HeLa cells. The fluorescence signal comes from TAMRA dye-modified DNA reporter probes, and the images were taken by an Olympus FV500-IX81 confocal microscope (Olympus America, Melville, NY).
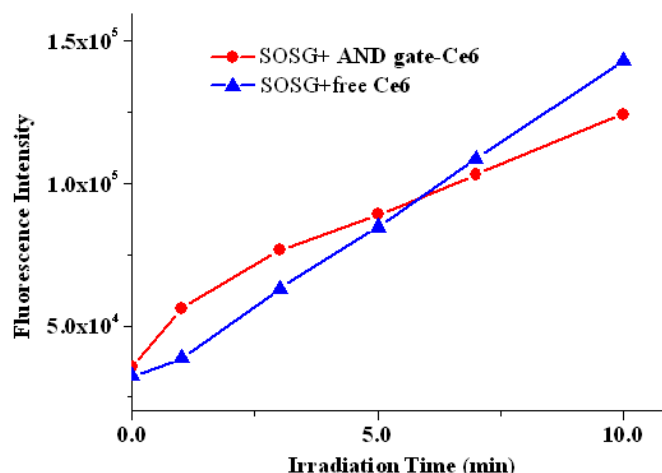
Figure S5. Ce6-mediated singlet oxygen generation after white light irradiation, as demonstrated by detecting singlet oxygen sensor green (SOSG) fluorescence. The free Ce6 and oligonucleotide-modified Ce6 displayed similar singlet oxygen generation efficiency for photodynamic therapy, while without Ce6, no obvious SOSG fluorescence change was detected (data not shown). To extend the lifetime of the generated singlet oxygen, 10 µM Ce6 probe and 2.0 µM SOSG were introduced within each 200 µL of D_2O solution, and the fluorescence intensity was read using excitation at 504 nm and maximum emission at 525 nm.
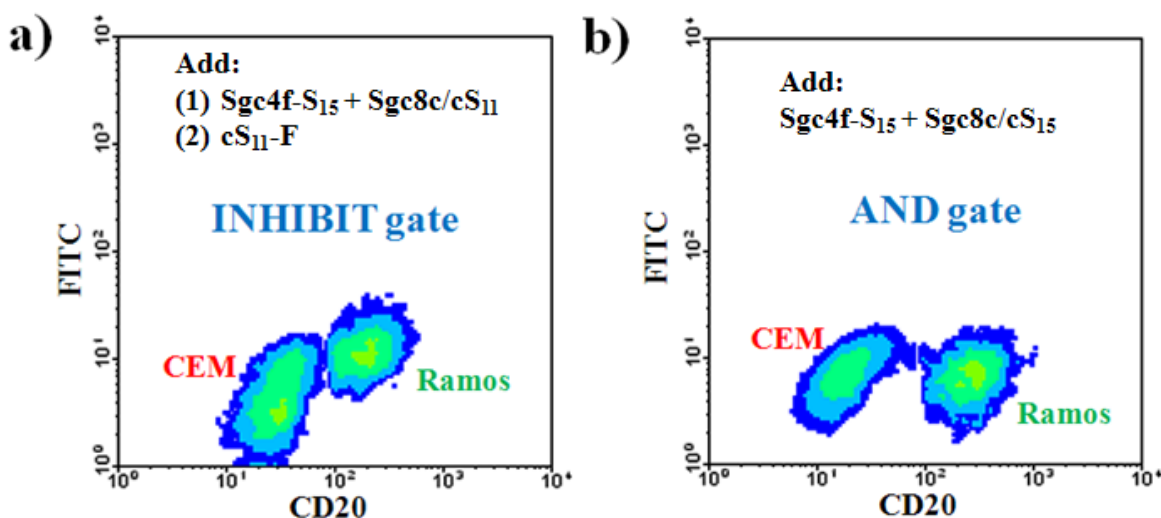

Figure S6. Mixed cell experiments. Tagged aptamer probe Sgc4f-S_{15} and aptamer-duplex conjugation for the aptamer-switch-based **AND** gate and **INH** gate (Sgc8c/cS$_{15}$-FAM and Sgc8c/cS$_{11}$, respectively) were incubated at a concentration of 200 nM with a mixture of 10^6/ mL Ramos and CEM cells in 200 µL binding buffer on ice and shaken for 1 hour. After washing and discarding the nonbinding probes, 100 nM FAM-labeled cS$_{11}$ reporter probe was added for 1

hour of strand binding and incubation on ice. After further washing to remove nonbinding probes, the final detection of cellular fluorescence signal was performed with a FACScan cytometer by counting 20 000 events, using channel #3 for the FITC dye and channel #5 for the PE-Cy5.5 dye. PE-Cy5.5 dye was used to label biotinylated CD20 antibody to distinguish CEM and Ramos cells. CD20 antibody has been proven not to compete with the binding site of either Sgc8c or Sgc4f aptamer. For the INH gate, the binding of Sgc8c on the CEM cell membrane will release cS_{11} to inhibit the binding of additional cS_{11}-F reporter. This effect was observed to result in a decreased signal mainly from the CEM cells. This may be explained by the high local concentration of released cS_{11} strand near CEM cells, which was recaptured by the portion of Sgc4f-S_{15} strand bound on the CEM cell membrane. The high FITC fluorescence signal for the AND gate Ramos cells results partially from the relatively high background signal of cells only.
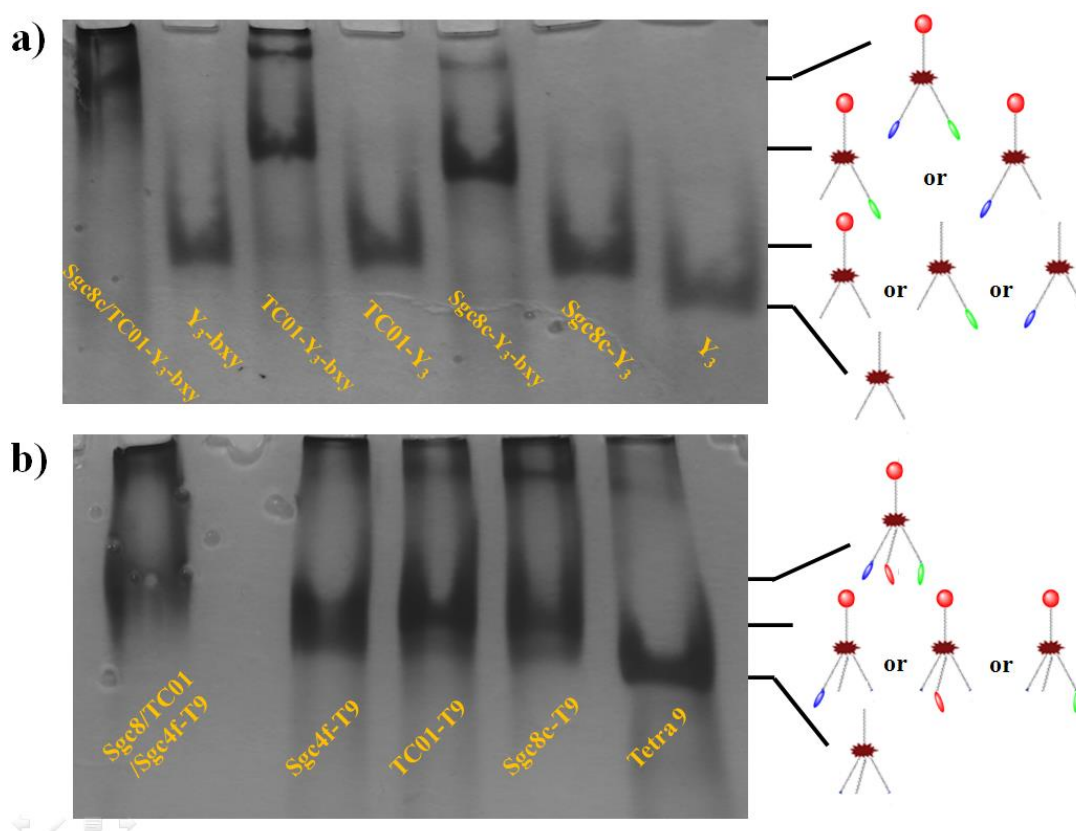

Figure S7. "Nano-Claw" constructed for simultaneous recognition of multiple cell-surface markers. Native gel electrophoresis studies confirmed the expected reporting mechanism and the successful construction of the "Nano-Claw".
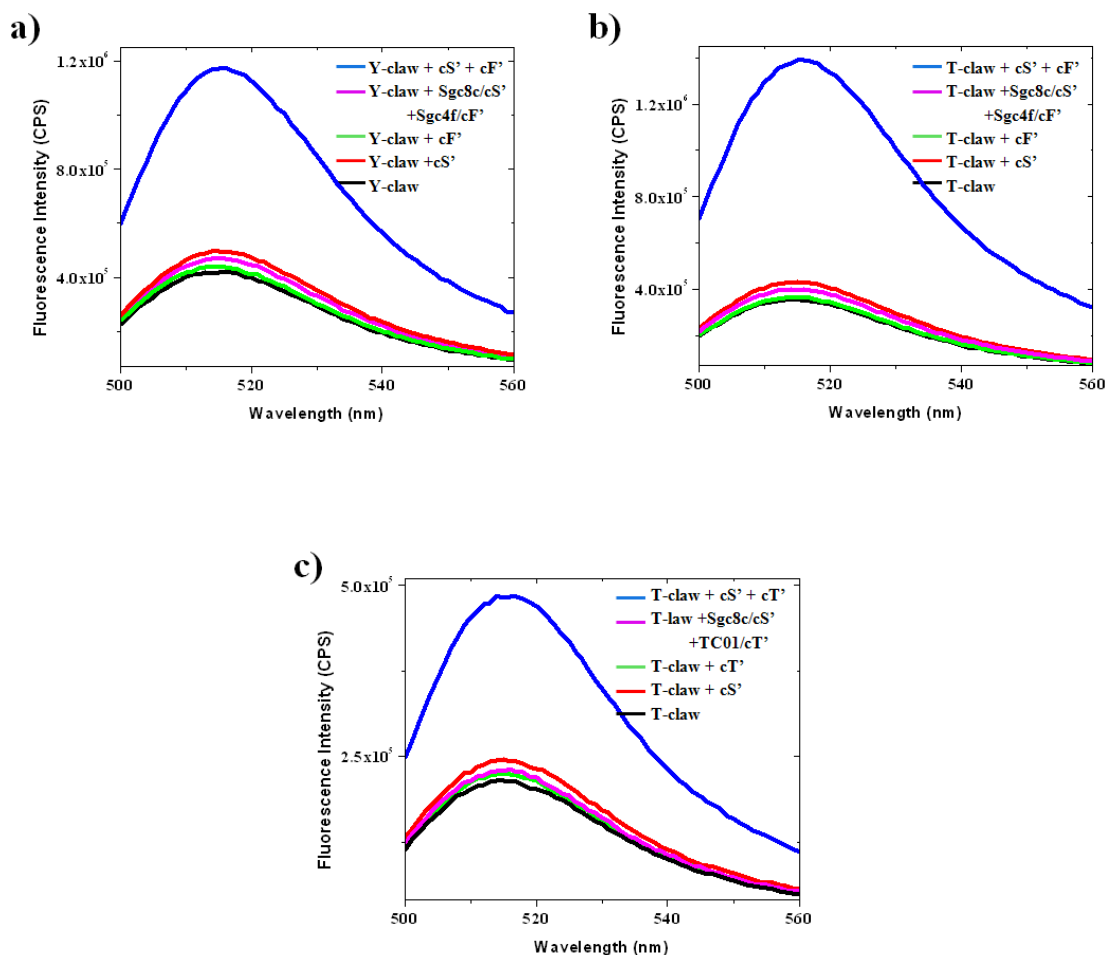
Figure S8. Fluorescence studies proving the signaling property of the "Nano-Claw". The fluorescence intensity was recorded for FAM-R- and Dabcyl-cS'-strand-modified trivalent "Y"-shaped and tetravalent "X"-shaped claws, λ_{ex}= 488 nm. The FAM fluorescence was recovered only in the presence of both free cS' and cT' strands (the blue curve); in contrast, the addition of any single free strand (red or green) or aptamer-conjugated strands (pink) could not restore the signal. The fluorescence was measured after 20 minutes of incubation, with each probe concentration at 100 nM.
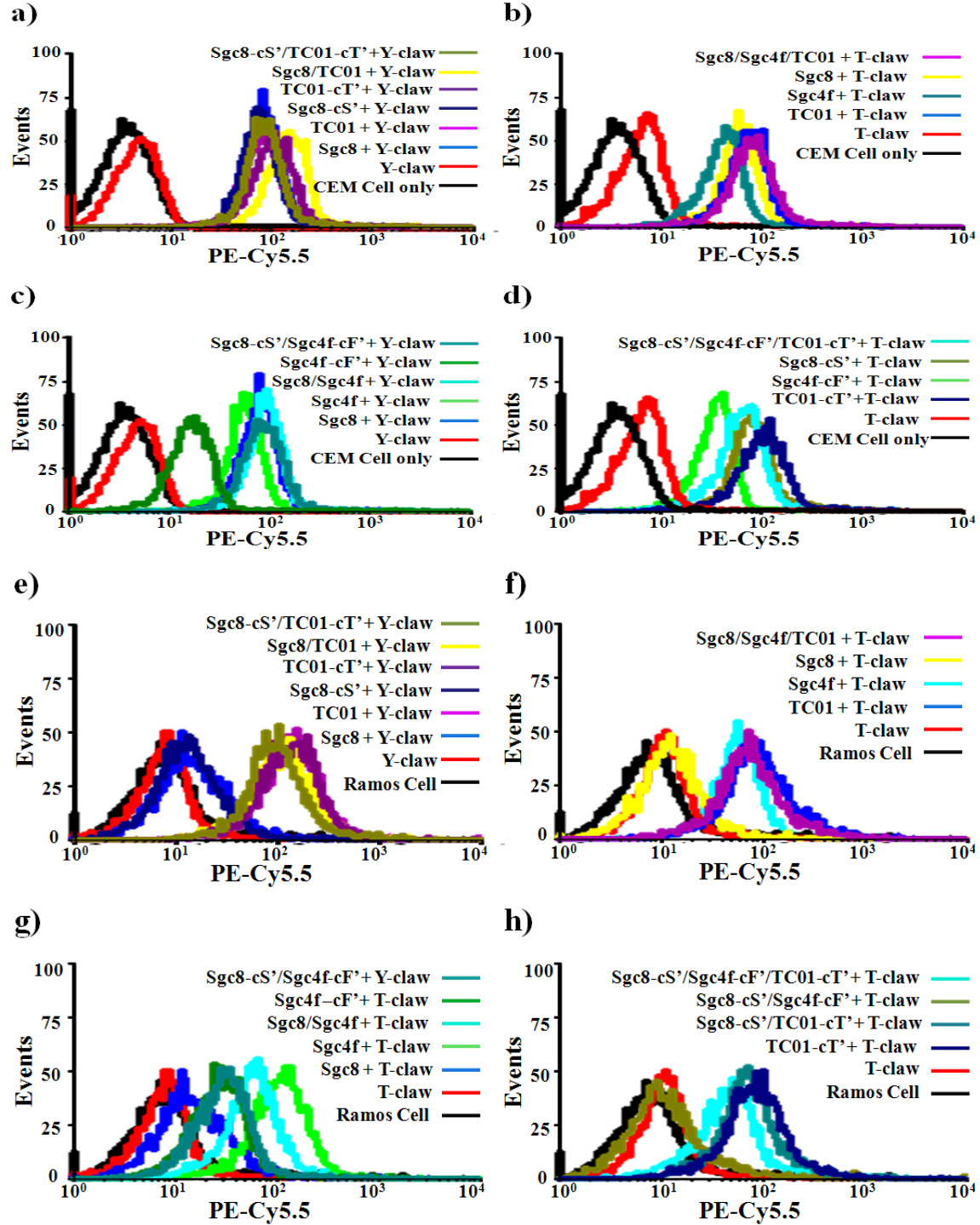
Figure S9. Persistence of the aptamer selectivity within the "Nano-Claw" construction. The expected specific binding of (**a, e**) Sgc8c/TC01-"Y" claw, (**c, g**) Sgc8c/Sgc4f-"Y" claw, and (**b, d, g, h**) Sgc8c/Sgc4f/TC01-"X" claw with CEM and Ramos cells was proven. The streptavidin-conjugated PE-Cy5.5 dye was used to stain the biotin-labeled R strand for labeling each claw construction.
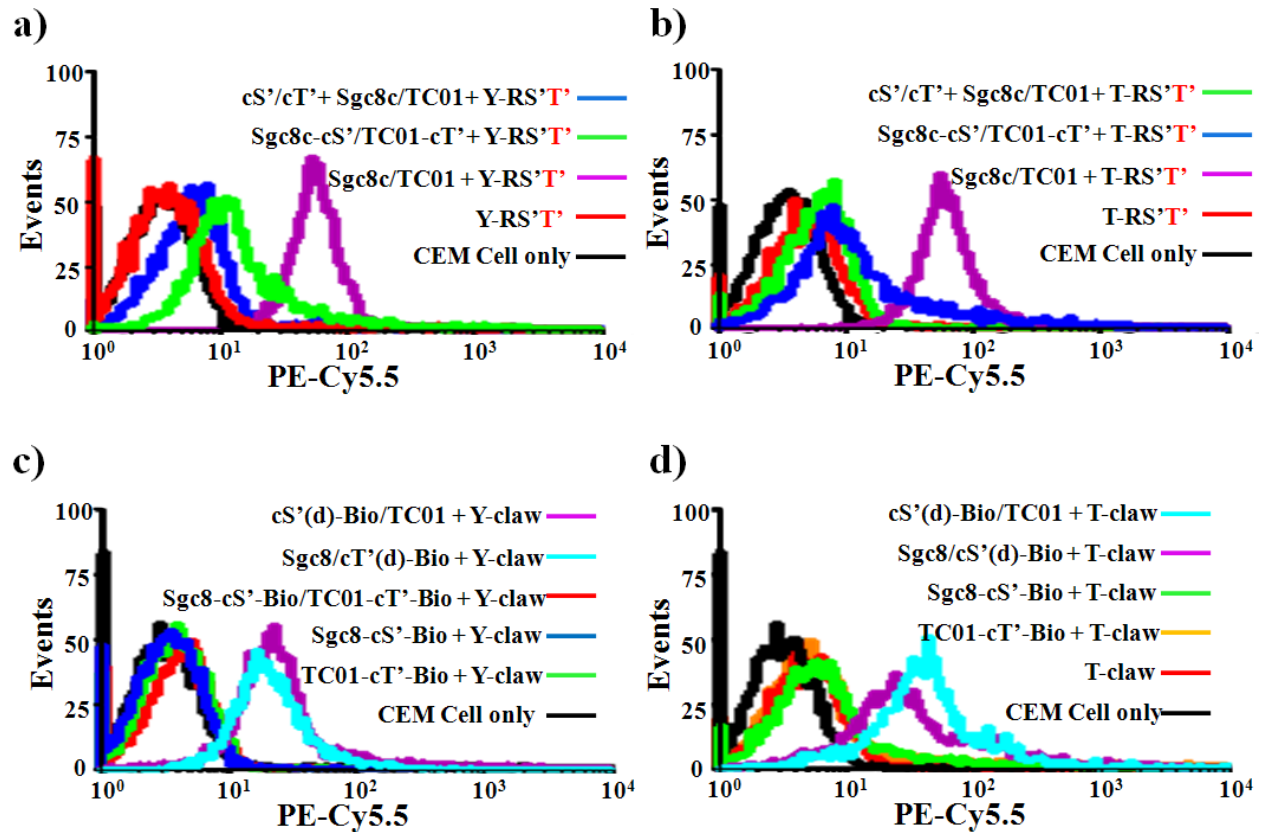
Figure S10. More evidence demonstrating the proper function of the "Nano-Claw". Biotin-labeled y strand (called y' in the figure) was used to prove the expected displacement within the (**a**) "Y"-shaped claw and (**b**) "X"-shaped claw. The left shift of the PE-Cy5.5 signal was observed when free cT' strand was induced, such as the green or blue curve. (**c, d**) Furthermore, biotin-labeled cS' or cT' strand was employed to track the status of these strands during the claw capture process. Once these strands are displaced by the cell-surface marker, a low fluorescence signal will be induced.
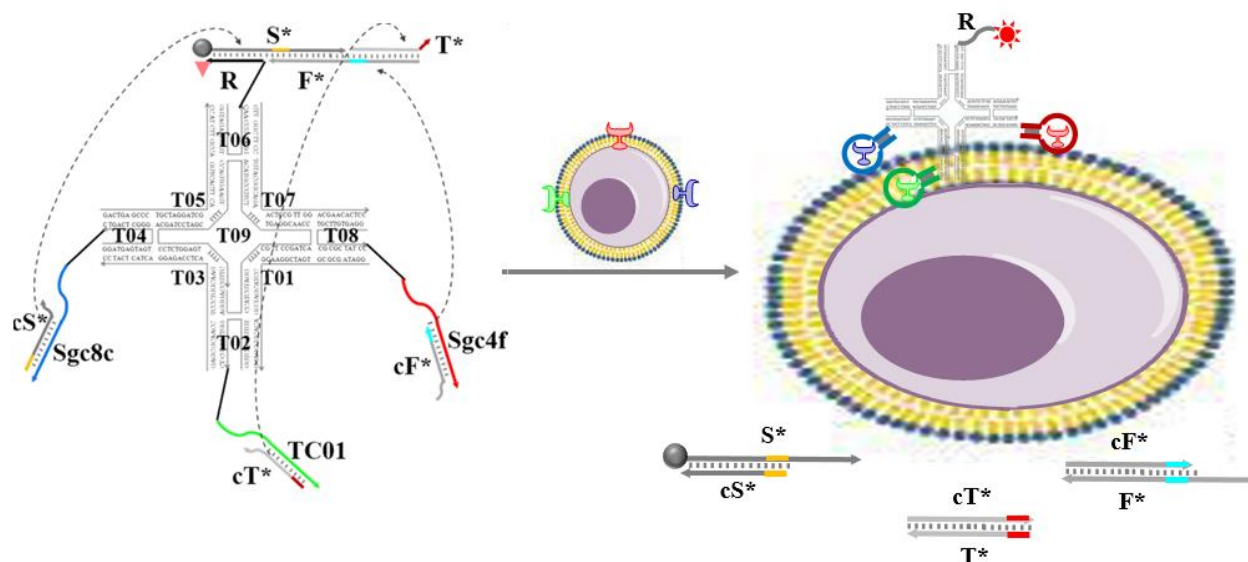
Figure S11. The construction scheme for 3-input tetravalent "X"-shape Nano-Claw. Similar mechanism can be expected for 2-input trivalent "Y"-shape Nano-Claw.
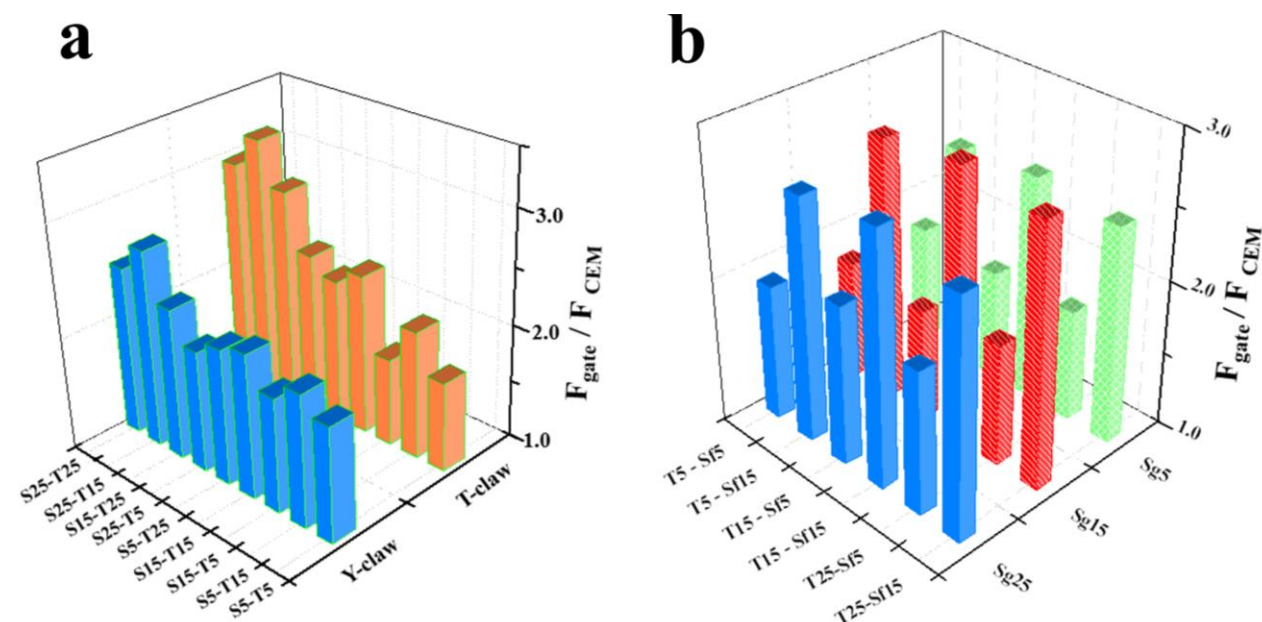

Figure S12. Effect of the "poly-T" linker length on the functions of the (**a**) "Y"- or "X"-shaped claw with two capture toes and (**b**) "X"-shaped claw with three capture toes. The fluorescence values were calculated based on the distributions in the flow cytometer from three experiments.

References:

 (1) Lee, J. B.; Roh, Y. H.; Um, S. H.; Funabashi, H.; Cheng, W.; Cha, J. J.; Kiatwuthinon, P.; Muller, D. A.; Luo, D. *Nat Nanotechnol* **2009**, *4*, 430.
 (2) Yan, H.; Park, S. H.; Finkelstein, G.; Reif, J. H.; LaBean, T. H. *Science* **2003**, *301*, 1882.
 (3) Puglisi, J. D.; Tinoco, I. *Methods Enzymol* **1989**, *180*, 304.